On the robustness of the ammonia thermometer

S. Maret, A. Faure, E. Scifoni, L. Wiesenfeld

Mon. Not. R. Astron. Soc. **399,** 425–431 (2009) doi:10.1111/j.1365-2966.2009.15294.x

On the robustness of the ammonia thermometer

S. Maret,[1⋆] A. Faure,[1] E. Scifoni[1,2] and L. Wiesenfeld[1]

[1] *Laboratoire d'Astrophysique de Grenoble, Observatoire de Grenoble, Université Joseph Fourier, CNRS, UMR 5571 Grenoble, France*
[2] *Frankfurt Institute for Advanced Studies, Johann Wolfgang Goethe University, Frankfurt am Main, Germany*

Accepted 2009 June 22. Received 2009 June 22; in original form 2009 April 30

ABSTRACT

Ammonia inversion lines are often used as probes of the physical conditions in the dense interstellar medium. The excitation temperature between the first two para-metastable (rotational) levels is an excellent probe of the gas kinetic temperature. However, the calibration of this ammonia thermometer depends on the accuracy of the collisional rates with H_2. Here, we present new collisional rates for ortho- and para-NH_3 colliding with para-$H_2(J = 0)$, and investigate the effects of these new rates on the excitation of ammonia. Scattering calculations employ a new, high-accuracy, potential energy surface computed at the coupled-cluster CCSD(T) level with a basis set extrapolation procedure. Rates are obtained for all transitions involving ammonia levels with $J \leq 3$ and for kinetic temperatures in the range 5–100 K. We find that the calibration curve of the ammonia thermometer – which relates the observed excitation temperature between the first two para-metastable levels to the gas kinetic temperature – does not change significantly when these new rates are used. Thus, the calibration of ammonia thermometer appears to be robust. Effects of the new rates on the excitation temperature of inversion and rotation–inversion transitions are also found to be small.

Key words: molecular data – molecular processes – ISM: molecules.

1 INTRODUCTION

Since its discovery in the interstellar medium 40 years ago by Cheung et al. (1969), ammonia has been widely used as a probe of the physical conditions in a variety of interstellar environments, ranging from pre-stellar cores, molecular clouds, to external galaxies(see Ho & Townes 1983 for a review). The peculiar structure of the molecule makes ammonia lines excellent tracers of the density and temperature in these environments. NH_3 is a symmetric top molecule, whose rotational levels can be denoted by two quantum numbers, the total angular momentum J and its projection K along the C_{3v} molecular axis. Owing to the possible relative orientations of the hydrogen spins, two distinct species exist: ortho-NH_3 (o-NH_3; $K = 3n$, with n being an integer) and para-NH_3 (p-NH_3; $K \neq 3n$). As both radiative and non-reactive collisional transitions do not change the spin orientations, transitions between o- and p-NH_3 are forbidden. Each of the rotational energy levels (with the exception of those with $K = 0$) is further split into two sublevels which can be denoted either by the inversion symmetry of the vibrational wave functions or by the symmetry index $\epsilon = \pm 1$ (see fig. 1 and equation 29 in Rist, Alexander & Valiron 1993).[1] This splitting is caused by the inversion motion of the molecule, and the corresponding inversion transitions fall in the range $\lambda \sim 1$ cm. Electric dipole transition rules ($\Delta J = 0, \pm 1$, $\Delta K = 0$) prevent radiative transitions between different K ladders to occur. Consequently, the lowest inversion doublets in each K ladder (i.e. with $J = K$) are metastable; they can be relaxed only through collisions.

For this reason, the relative population of the first two metastable inversion doublets of p-NH_3, $J_{K,\epsilon} = 1_{1,\pm}$ and $2_{2,\pm}$, depends solely on the kinetic temperature. Considering only the first three doublets, $1_{1,\pm}$, $2_{2,\pm}$ and $2_{1,\pm}$, and assuming that the population of the $2_{1,\pm}$ doublet is much smaller than that of the $2_{2,\pm}$, Walmsley & Ungerechts (1983) showed that the excitation temperature between the two lowest doublets is given by the analytic formula

$$T_{1,2}^{A} = T \left\{ 1 + \frac{T}{T_0} \ln \left[1 + \frac{C\,(2_2 \rightarrow 2_1)}{C\,(2_2 \rightarrow 1_1)} \right] \right\}^{-1}, \quad (1)$$

where T_0 is the energy difference between the first two metastable doublets ($\sim$41.7 K), T is the kinetic temperature, $C(2_2 \rightarrow 2_1)$ is the collisional excitation rate (averaged over the symmetry index ϵ) between the $J_K = 2_2$ and 2_1 rotational levels, and $C(2_2 \rightarrow 1_1)$ is the collisional de-excitation rate between the 2_2 and 1_1 levels. Thus, if one knows the $T_{1,2}$ excitation temperature, one can derive the kinetic temperature of the gas, effectively using ammonia inversion lines as a 'thermometer'.

Observationally, $T_{1,2}$ can be determined by observing the hyperfine components of the $1_{1,-} \rightarrow 1_{1,+}$ and $2_{2,+} \rightarrow 2_{2,-}$ inversion transitions. The inversion doublets have indeed hyperfine components, which are due to the interaction between the electric quadrupole moment of the N nucleus and the electric field gradient created

⋆E-mail: sebastien.maret@obs.ujf-grenoble.fr

[1] In this paper, we denote each level by its symmetry index ϵ, with a '+' sign for $\epsilon = +1$ and a '−' sign for $\epsilon = -1$. We refer the reader to fig. 1 of Rist et al. (1993) for an energy diagram of the molecule.

by the electrons. If one assumes that the excitation temperature of each hyperfine components (within a given rotational state) is the same, then one can derive the opacity $\tau(1_1)$ and $\tau(2_2)$ of the 1_1 and 2_2 multiplets from the relative intensity of each hyperfine component (Barrett, Ho & Myers 1977). $T_{1,2}$ is then calculated from the following formula (Ho et al. 1979; Hotzel, Harju & Juvela 2002):

$$T_{1,2} = -T_0 \Big/ \ln\left[\frac{9}{20}\frac{\tau(2_2)}{\tau(1_1)}\right]. \quad (2)$$

In order to 'calibrate' the ammonia thermometer, i.e. to compute the kinetic temperature from the measured $T_{1,2}$ excitation temperature, good knowledge of the collisional rates of NH_3 colliding with H_2 is necessary (see equation 1). Although a large number of measurements have been made on the NH_3–H_2 system, using in particular double resonance (e.g. Daly & Oka 1970), crossed beam (e.g. Schleipen, ter Meulen & Offer 1993) and pressure broadening (e.g. Willey et al. 2002) experiments, laboratory data generally do not directly provide state-to-state rate coefficients. As a result, radiative transfer models can exclusively rely on theoretical estimates. On the other hand, laboratory measurements are crucial to establish the predictive abilities of theory and, in particular, of the potential energy surfaces (PES).

Following the pioneering work of Morris et al. (1973), Walmsley & Ungerechts (1983) performed statistical equilibrium calculations based on the theoretical NH_3–He collisional rates of Green (1980). Danby et al. (1988) then determined more accurate collisional rates for collisions of NH_3 with p-H_2($J = 0$) and used them to recalibrate the ammonia thermometer. The scattering calculations of Danby et al. (1988) were based on the *ab initio* NH_3–H_2 PES of Danby et al. (1986). This latter was subsequently improved to investigate propensity rules at selected collisional energies for ammonia colliding with both p- and o-H_2 (Offer & Flower 1990; Rist et al. 1993). More recently, high-accuracy *ab initio* calculations have been performed by Mladenović et al. (2008) to explore the topographical features of the NH_3–H_2 interaction. In this paper, we present new collisional rates based on the determination of a new, highly accurate, NH_3–H_2 *ab initio* PES. Ammonia and hydrogen molecules are treated as rigid rotors, and H_2 is further constrained in the scattering calculations to be in the (spherically symmetrical) para-$J = 0$ state, as in Danby et al. (1988). Hence, the main difference between the present collisional rates and those of Danby et al. (1988) arises from the PES. These new rates are then used to estimate the robustness of the ammonia thermometer and the excitation of ammonia lines under the condition that prevails in cold molecular clouds, prestellar cores and protostars ($T < 100$ K). For this, we compute the excitation of both o- and p-NH_3 using a non-local thermodynamic equilibrium (non-LTE) radiative transfer code. This paper is organized as follows. In Section 2, we present both the new NH_3–H_2 PES and the scattering calculations. Our excitation computations and the comparison with earlier computations are presented in Section 3. Section 4 concludes this article.

2 POTENTIAL ENERGY SURFACE AND COLLISIONAL RATES

2.1 Potential energy surface

The ammonia and hydrogen molecules were both assumed to be rigid. This assumption is adequate here because (i) the investigated collisional energies are below the first vibrational excitation threshold of ammonia ($\nu_2 = 932.4$ cm^{-1}; Rajamäki et al. 2004) and (ii) the corresponding collision time-scales are much faster than the inversion motion of ammonia. Monomer geometries were taken at their ground-state average values, as recommended by Faure et al. (2005). The average structure of NH_3 was derived from the high-accuracy calculations of Rajamäki et al. (2004): $r_{NH} = 1.9512$ Bohrs, and $\widehat{HNH} = 107.^{\circ}38$. The ground-state average geometry of H_2 was taken as $r_{HH} = 1.4488$ Bohrs (e.g. Faure et al. 2005). The conventions of Phillips et al. (1994) were employed in defining the NH_3–H_2 rigid-rotor (five-dimensional) coordinate system [one H atom lies in the (x, z) plane].

The NH_3–H_2 PES was constructed using the following two step procedure: (i) a reference PES was computed from a large set (89 000 points) of CCSD(T)[2] calculations using Dunning's correlation consistent aug-cc-pVDZ basis set and (ii) this reference surface was calibrated using a complete basis set (CBS) extrapolation procedure based on a smaller set (29 000 points) of CCSD(T)/aug-cc-pVTZ calculations. A CBS-type extrapolation was applied to the correlation part of the interaction energy and was performed using a two-point X^{-3}-type extrapolation, where X is the cardinal number corresponding to the basis set, as described in Jankowski & Szalewicz (2005). The self-consistent field (SCF) contribution was not extrapolated but was taken at the aug-cc-pVTZ level. All basis sets were supplemented with mid-bond functions, and all calculations were counterpoise corrected as in Jankowski & Szalewicz (2005). The same strategy was recently applied to H_2CO–H_2 (Troscompt et al. 2009).

Grid points were chosen for 29 fixed intermolecular distances R (in the range 3–15 a_0) via random sampling for the angular coordinates of H_2 relative to NH_3. At each intermolecular distance, the interaction energy was then least-squares fitted using a 120-term expansion for the angular coordinates, using equation (3) of Phillips et al. (1994) adapted to the C_{3v} symmetry of NH_3. This expansion includes anisotropies up to $l_1 = 11$ and $l_2 = 4$, where the integer indices l_1 and l_2 refer to the tensor ranks of the angular dependence of the NH_3 and H_2 orientation, respectively. The CBS correction was fitted over a subset of only 46 angular terms with $l_1 \leq 7$ and $l_2 \leq 4$. We note that the expansion restricted to p-H_2($J = 0$), in which all terms with $l_2 \neq 0$ are eliminated, includes only 24 terms. The accuracy of the angular expansions was monitored using a self-consistent Monte Carlo error estimator. A cubic spline interpolation was finally employed over the whole intermolecular distance range and was smoothly connected with standard extrapolations to provide continuous radial expansion coefficients suitable for scattering calculations. Technical details on the fitting strategy can be found in Valiron et al. (2008). The accuracy of the final five-dimensional fit was found to be better than 1 cm^{-1} in the long-range and minimum region of the interaction ($R > 5$ Bohrs). The accuracy of the above procedure was also checked against a moderate set (1200 points) of 'high-cost' CCSD(T)–R12 calculations which offer a direct way of reaching the basis set limit value within a single calculation, i.e. without extrapolation (Noga & Kutzelnigg 1994). The rms error between the final fit and the benchmark CCSD(T)–R12 values was found to be lower than 1 cm^{-1} in the whole attractive part of the interaction ($R \geq 6$ Bohrs). We emphasize that the intrinsic accuracy of CCSD(T) calculations at the basis set limit is $\sim$1 cm^{-1}.

Constraining H_2 in its lowest para level ($J = 0$) is strictly equivalent to averaging the PES over the H_2 rotational motion. The global minimum of this averaged PES lies at -85.7 cm^{-1} for $R =$ 6.3 Bohrs, with H_2 in an almost equatorial location, equidistant

[2] CCSD(T) stands for the coupled-cluster method with non-iterative evaluation of triple excitations.

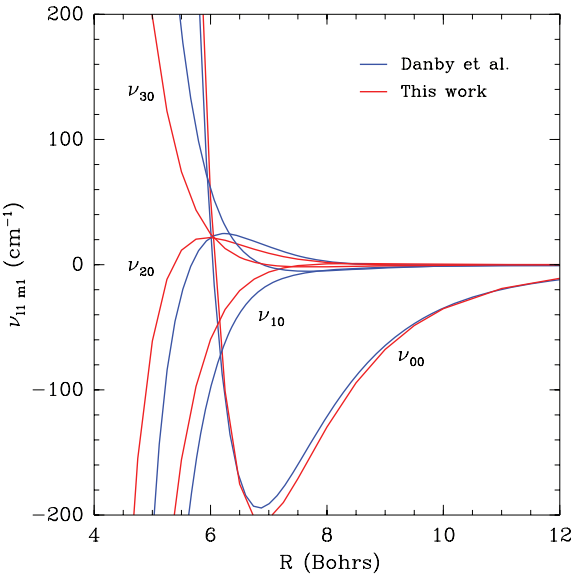

Figure 1. Comparison between the first four angular expansion coefficients, $v_{l_1 m_1}$, of the NH_3–H_2 PES (Danby et al. 1986) with those from the present work, as a function of the intermolecular distance R.

from the two closest H atoms of ammonia. A similar location was found for the global minimum of the NH_3–He interaction, but with a significantly more shallow potential well at ~ -33 cm^{-1} (Hodges & Wheatley 2001). The five-dimensional PES, including the anisotropy of H_2, is of course qualitatively different: the global minimum, as deduced from our fit, lies at -267 cm^{-1} for $R =$ 6.1 Bohrs, with H_2 co-linear with the C_{3v} axis of ammonia at the nitrogen end. It is interesting to compare this result with the recent calculations of Mladenović et al. (2008): these authors found the global minimum of the NH_3–H_2 interaction at a similar location with a comparable, although significantly smaller, binding energy (-253 cm^{-1}). As their calculations were performed at a similar level of accuracy [CCSD(T) method and aug-cc-pVQZ basis sets], this difference most likely reflects monomer geometry effects. Detailed comparisons will be investigated in dedicated future works.

Now, in order to compare the present NH_3–H_2 PES with that employed by Danby et al. (1988), we present in Fig. 1 a comparison of the angular expansion coefficients $v_{l_1 m_1}$. The definition of these coefficients is given in equation (2.1) of Danby et al. (1986) and their values are listed in their table 4.[3] Only the first four are plotted for clarity in the figure. Despite significant differences at short range ($R \leq 6$ Bohrs), the overall agreement between the two sets of coefficients is quite reasonable. This comparison (i) indicates the good quality of the *ab initio* calculations of Danby et al. (1986) and (ii) suggests moderate effects of the new PES on the dynamics, as shown below.

Finally, it should be noted that the PES of Danby et al. (1986) has been previously checked against laboratory measurements: Schleipen et al. (1993) and Willey et al. (2002) reported, respectively, symmetry-resolved state-to-state and broadening cross-sections. In both cases, a good overall agreement was obtained between theory and experiment, suggesting the adequacy of the PES. Discrepancies were however noted, in particular strong propensity rules predicted by the theory for NH_3–p-H_2 were observed in the experiment to a much lower extent (see below).

2.2 Scattering calculations

The quantal theory for scattering of a symmetric top with an atom or a structureless molecule like $H_2(J = 0)$ can be found in Green (1976). The extension of the formalism to the scattering of a symmetric top with a linear molecule can be found in Offer & Flower (1990) and Rist et al. (1993). In the present work, calculations were performed using the (non-reactive) scattering code MOLSCAT[4] in which the extension to allow for the rotational structure of H_2 is not yet implemented. Hence, the present calculations were restricted to collisions between NH_3 and p-$H_2(J = 0)$. Extension to p-$H_2(J =$ 0, 2) and o-$H_2(J = 1)$ is under way and is further discussed below.

All calculations were performed at the close-coupling level. Inversion doubling was neglected, and the inversion-tunnelling wavefunction was simply taken as a linear combination of two delta functions centred at the equilibrium position (Green 1976; Davis & Boggs 1978). We actually tested this approximation on the NH_3–He system by taking the inversion coordinate explicitly into account, as done previously by Davis & Boggs (1981). To this aim, we employed the high-quality NH_3–He PES of Hodges & Wheatley (2001), which does include the inversion dependence of the interaction. The inversion motion was found to have a negligible effect (less than 10 per cent) on the rigid-body interaction potential and on the cross-sections (Scifoni et al. 2007), as was concluded by Davis & Boggs (1981) from a lower quality potential. We note that van der Sanden et al. (1992) obtained a comparable result for the NH_3–Ar interaction. A similar conclusion is therefore expected for the NH_3–H_2 interaction, although the inversion dependence of this PES is yet not known.

We adopted the rotational constants $A = B = 9.944\,116$ cm^{-1} and $C = 6.228\,522$ cm^{-1}. The reduced mass of the system is 1.802 289 amu. As the ortho and para levels of ammonia do not interconvert in inelastic collisions, these were treated separately. The coupled-channel equations were integrated using the modified log-derivative propagator of Manolopoulos (1986). The radial propagation used a step size parameter STEPS = 10 except at total energies below 30 cm^{-1} where STEPS was increased up to 300 to constrain the step length of the integrator below $\sim$0.1 Bohrs. Other propagation parameters were taken as the MOLSCAT default values. Calculations were performed for collision energies between $\sim$0.1 and 700 cm^{-1}. The energy grid was adjusted to reproduce all the details of the resonances, with an energy step of 0.2 cm^{-1} up to total energies of 150 and 0.5 cm^{-1} from 150 to 300 cm^{-1}. All calculations also included several energetically closed channels to ensure that cross-sections were converged to within 7–8 per cent for all transitions involving $J \leq 3$. Thus, at the highest investigated energies, the basis set incorporated all target states with $J \leq 11$ and 12 for o- and p-NH_3, respectively.

Excitation cross-sections for o-NH_3 are presented in Fig. 2 for rotation–inversion transitions out of the ground state of o-NH_3. Prominent resonant features are observed in this plot. These are caused by both Feshbach- and shape-type resonances. It should be noted that only Feshbach-type resonances are observed in NH_3–He collisions (e.g. Machin & Roueff 2005). This difference between He and $H_2(J = 0)$ reflects the deeper potential well of the NH_3–H_2 PES, as discussed in Section 2.1. Resonances are found to significantly increase the cross-sections at low energy and, therefore, the rate coefficients at low temperature. For example, at 10 K, the NH_3–H_2 rate coefficient for the ground-state transition of o-NH_3 $1_{0,+} \rightarrow 0_{0,+}$

[3] $v_{l_1 m_1}$ corresponds to $v_{\lambda\mu}$ in equation (2.1) of Danby et al. (1986).

[4] http://www.giss.nasa.gov/tools/molscat

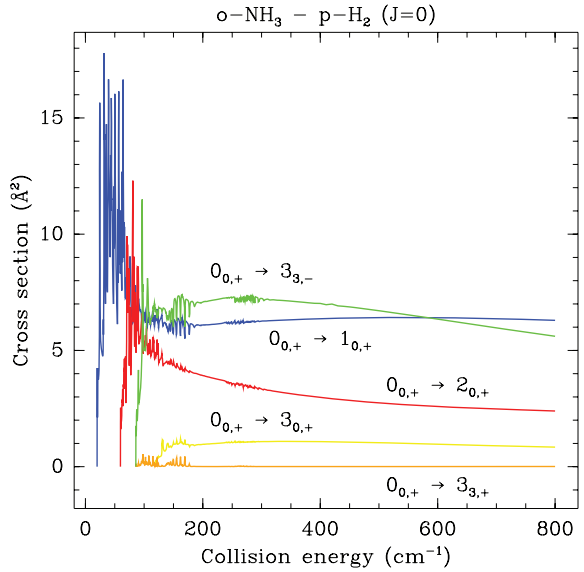

Figure 2. Cross-sections for transitions out of the $0_{0,+}$ rotational level of o-NH_3 into levels $J_{K,\epsilon}(J \leq 3)$ as a function of collision energy.

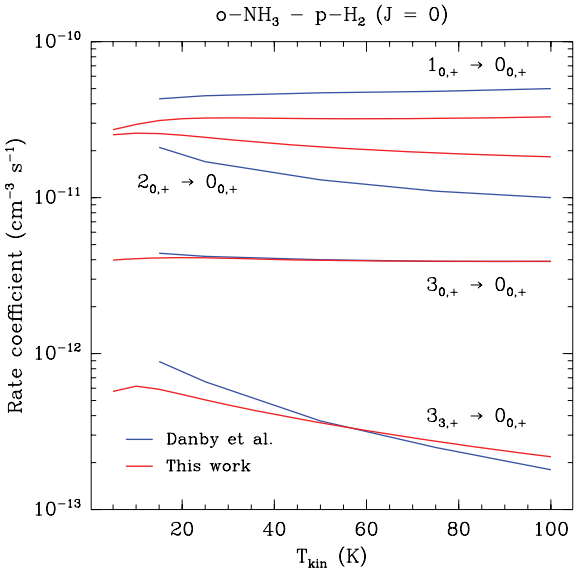

Figure 3. Comparison between rate coefficients for collisional de-excitation of o-NH_3 by p-$H_2(J = 0)$ of Danby et al. (1986) and those from this work, as a function of temperature. Only transitions towards the ground state $0_{0,+}$ are displayed.

is a factor of 20 larger than the NH_3–He rate of Machin & Roueff (2005). We note, however, that this factor reduces to 2.5 for the transition $2_{0,+} \rightarrow 0_{0,+}$ at the same temperature. Willey et al. (2002) also reported significant differences (up to a factor of 4) between p-H_2 and He broadening cross-sections. It is also noted that the cross-section for the $0_{0,+} \rightarrow 3_{3,+}$ transition is much lower than for $0_{0,+} \rightarrow 3_{3,-}$. This propensity rule was already observed in earlier calculations (Offer & Flower 1990; Rist et al. 1993) but, interestingly, it was found to be considerably weakened for collisions with o-$H_2(J = 1)$ and was observed experimentally only to a slight extent (Schleipen et al. 1993). On the other hand, it was found to be preserved when including the $J = 2$ state in the p-H_2 basis set (Offer & Flower 1990; Rist et al. 1993). This inclusion was also found to change the absolute values of the cross-sections, at a few selected energies, by up to a factor of 3 (Offer & Flower 1990; Rist et al. 1993). Its effect on the average cross-sections and rate coefficients is however expected to be moderate, typically 20–30 per cent. This was indeed checked in the case of ND_2H–H_2 calculations employing the present PES (Scifoni et al., in preparation). As a result, the rate coefficients presented below are expected to be accurate within typically 30 per cent.

Cross-sections were integrated over Maxwell–Boltzmann distributions of collisional velocities, and collisional rate coefficients were obtained in the range 5–100 K for all transitions involving ammonia levels with $J \leq 3$ (the lowest levels with $J = 4$ lie at 177 and 237 K above the ground states of p- and o-NH_3, respectively). Higher levels and temperatures were not investigated in the present work because collisional rates with o-H_2 are required in models considering temperatures above 100 K. These collisional rate coefficients are made available in the BASECOL[5] and LAMBA[6] data bases as well as at the CDS.[7]

In Fig. 3, downward rate coefficients are presented for rotation–inversion transitions towards the ground state. The resonant features are found to be completely washed out by the thermal average. The

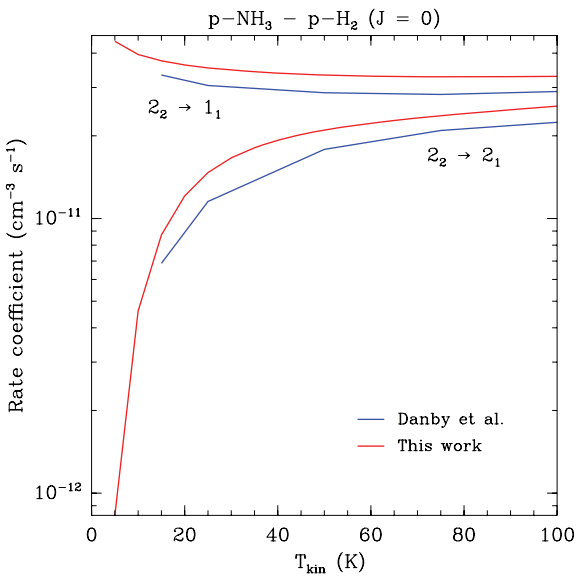

Figure 4. Comparison between the rate coefficients for collisional excitation and de-excitation of p-NH_3 by p-$H_2(J = 0)$ of Danby et al. (1986) and those from this work, as a function of temperature. These rates have been averaged over the symmetry index ϵ.

present results are compared with the data of Danby et al. (1988). As expected from the comparison of the expansion angular coefficients (see Fig. 1), the new rates agree within a factor of 2 with those of Danby et al. (1988). We see, however, that there is no particular trend, although the present rates are generally larger.

In Fig. 4, we show the symmetry-averaged rates $C(2_2 \rightarrow 2_1)$ and $C(2_2 \rightarrow 1_1)$ that appears in equation (1), as a function of the temperature. The new rates are found to be larger than those of Danby et al. (1988) by typically 15 per cent but closely follow the same temperature dependence. As a result, minor modifications of the ammonia thermometer are expected, as shown below.

[5] http://www.obspm.fr/basecol/
[6] http://www.strw.leidenuniv.nl/ moldata/
[7] http://cdsweb.u-strasbg.fr/

3 NON-LTE EXCITATION COMPUTATIONS

In order to estimate the effect of the new collisional rates on the calibration of the ammonia thermometer, we have computed the excitation of both o- and p-NH_3 using the large velocity gradient code of van der Tak et al. (2007). We have used the o- and p-NH_3 collisional rates with p-H_2 presented in the previous section, as well as those from Danby et al. (1988), for comparison. The latter were taken from the LAMBA data base (Schöier et al. 2005). Collision between NH_3 and He was neglected, because, in addition to H_2 being more abundant than He by a factor of 5, NH_3–H_2 collision rates are typically a factor of 3 larger than the NH_3–He rates (Machin & Roueff 2005). Energy levels, statistical weights and Einstein coefficients were taken from the JPL data base for molecular spectroscopy (Pickett et al. 1998). For the calculations using Danby et al. (1988) collisional rates, the first 24 levels of o-NH_3 and the first 17 levels of p-NH_3 were considered (corresponding to energy levels up to 416 and 297 cm^{-1}, respectively). For the calculations using the new rates, only the first six levels of o-NH_3 and the first 10 levels of p-NH_3 were considered (up to 118 and 115 cm^{-1}, respectively). In both cases, we have neglected the hyperfine structure of the molecule, i.e. we have considered that each hyperfine level within a given inversion level corresponds to the same energy level. While this hypothesis will lead to an overestimate of the line opacity for optical depths greater than a few, it is valid if the line is optically thin (Daniel, Cernicharo & Dubernet 2006). We have therefore chosen a column density to velocity gradient ratio that is large enough for this approximation to be valid [$N(NH_3)/(dv/dr) = 10^{-4}\,cm^{-3}/(km\,s^{-1}\,pc^{-1})$; the same value adopted by Walmsley & Ungerechts (1983)].

Fig. 5 shows the excitation temperature between the 1_1 and 2_2 metastable levels computed using both sets of collisional rates and as a function of the kinetic temperature. This excitation temperature is obtained by summing the populations of the $\epsilon = +1$ and -1 within each rotational state. A p-H_2 density of $10^4\,cm^{-3}$ was assumed. On this figure, we also show the excitation temperature computed from equation (1), i.e. assuming that only the first three

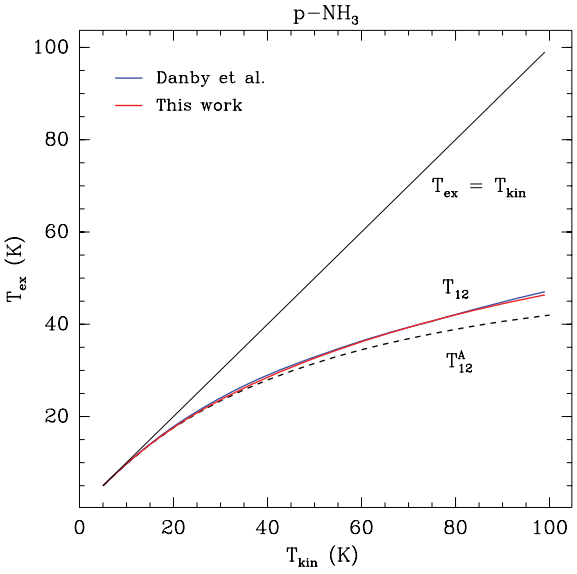

Figure 5. Rotational temperature between the 1_1 and 2_2 metastable levels of p-NH_3 computed using the collisional rates of Danby et al. (1988) and those from this paper, as a function of the kinetic temperature. The dashed curve shows the rotational temperature computed from equation (1).

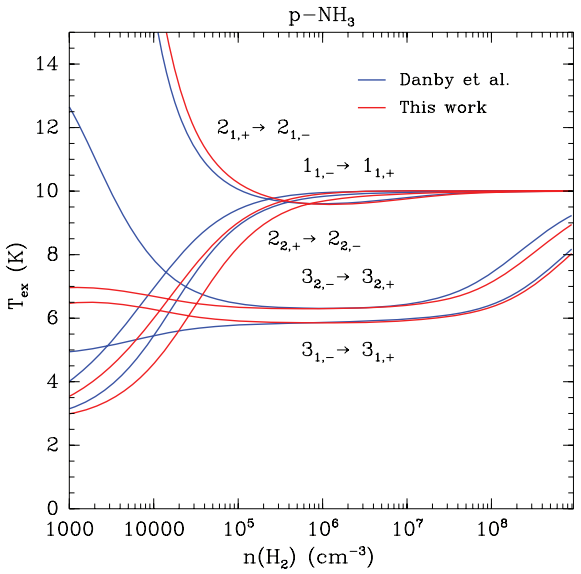

Figure 6. Excitation temperature of the p-NH_3 inversion transitions computed using the collisional rates of Danby et al. (1988) and those from this paper, as a function of the H_2 density. A kinetic temperature of 10 K is assumed.

rotational levels are populated. As seen on this figure, the excitation temperature computed using the rates of Danby et al. (1988) and the one computed using the rates presented in this paper agree extremely well; both values differ by less than 2 per cent. We also note that for kinetic temperatures lower than 20 K, the excitation temperature is well approximated by equation (1), but it underestimates it at larger temperature, because higher energy levels start to become populated. The good agreement between the kinetic temperature obtained using the rates of Danby et al. (1988) and those presented in this paper can be simply understood by the examination of equation (1). In this approximation, the excitation temperature depends on $\ln(1 + C_{21}/C_{23})$. Although the rates computed in this paper differ by ∼15 per cent with respect to those of Danby et al. (1988), their ratio (and a fortiori the logarithm of their ratio) differ much less. Therefore, the relation between the excitation temperature and the kinetic temperature – or in other words the calibration of the ammonia thermometer – appears to be robust.

Fig. 6 shows excitation temperature of several p-NH_3 inversion transitions, as a function of the density, for a kinetic temperature of 10 K and the same column density and line velocity than in Fig. 5. Spectroscopic data and critical densities are given in Table 1. For a multilevel system, the critical density can be defined (in the optically thin case) as the density at which the sum of the collisional de-excitation rates out of a given level is equal to the sum of the spontaneous radiative de-excitation rates:

$$n_{\rm crit}(T) = \frac{\sum_{J'_{K',\epsilon'}} A(J_{K,\epsilon} \rightarrow J'_{K',\epsilon'})}{\sum_{J'_{K',\epsilon'}} C(J_{K,\epsilon} \rightarrow J'_{K',\epsilon'})(T)}, \quad (3)$$

where the summation is done over the $J'_{K'\epsilon'}$ levels (with energies smaller than that of the $J_{K,\epsilon}$ considered). With this definition, the critical density refers to a level, and not to a transition.

For densities lower than $10^3\,cm^{-3}$, the excitation temperature of the $1_{1,-} \rightarrow 1_{1,+}$ and $2_{2,+} \rightarrow 2_{2,-}$ inversion transitions computed using the rates presented here and those of Danby et al. show little differences. For these densities, collisional de-excitation is negligible, and the excitation temperature of these lines is close to the background temperature (2.73 K). For densities much greater

Table 1. Frequencies, upper level energies and critical densities of the p- and o-NH_3 inversion and rotation–inversion transitions considered in this paper. Spectroscopic data are from the JPL catalogue. Energies are relative to the fundamental rotation–inversion level of each species, i.e. $1_{1,+}$ for p-NH_3 and $0_{0,+}$ for o-NH_3. The critical densities are given for a kinetic temperature of 10 K. They are computed using equation (3), and thus refer to the upper of level of the transition.

Species	Transition $J_{K,\epsilon} - J'_{K',\epsilon'}$	ν (GHz)	E_{up} (K)	n_{crit} (cm^{-3})
p-NH_3	$1_{1,-} \rightarrow 1_{1,+}$	23.694 496	1.1	3.90×10^3
p-NH_3	$2_{2,+} \rightarrow 2_{2,-}$	23.722 633	42.3	3.08×10^3
p-NH_3	$2_{1,+} \rightarrow 2_{1,-}$	23.098 819	58.3	1.44×10^8
p-NH_3	$3_{2,-} \rightarrow 3_{2,+}$	22.834 185	128.1	3.01×10^8
p-NH_3	$3_{1,-} \rightarrow 3_{1,+}$	22.234 506	144.0	5.41×10^8
o-NH_3	$3_{3,-} \rightarrow 3_{3,+}$	23.870 129	123.6	2.63×10^3
o-NH_3	$1_{1,+} \rightarrow 0_{0,+}$	572.498 068	27.5	5.45×10^7

than the critical density (i.e. $\gtrsim 10^6$ cm^{-3}), collisional de-excitation dominates, and lines are essentially thermalized. At intermediate densities, the $1_{1,-} \rightarrow 1_{1,+}$ and $2_{2,+} \rightarrow 2_{2,-}$ line excitation temperatures predicted using the rates from this work are slightly lower than the one predicted using those from Danby et al. This is because the de-excitation rates from this work are smaller (by about a factor of 2) than those of Danby et al. for these lines. As a consequence, the critical densities of the corresponding levels are greater than previously estimated, and the transition thermalizes at greater densities. Larger differences in the excitation temperatures of the $3_{2,-} \rightarrow 3_{2,+}$ and $3_{1,-} \rightarrow 3_{1,+}$ transitions – for which critical densities are a few 10^8 cm^{-3} – are seen. For example, at a density of 10^3 cm^{-3}, the excitation temperature of the $3_{2,-} \rightarrow 3_{2,+}$ transition computed using the rates of Danby et al. is almost a factor of 2 larger than the one computed with the rates obtained here. From the observer point of view, this has no consequences because the energy of the upper level of the transition is 123.6 K. At low densities, for the kinetic temperature considered here, the fractional population of this level is extremely small, and the predicted antenna temperature is essentially zero.

Fig. 7 shows the excitation temperature of the o-NH_3 $3_{3,-} \rightarrow 3_{3,+}$ inversion transition as a function of the density, for the same column density to velocity gradient ratio than in Fig. 6, but – since the upper level of the transition lies at ∼124 K above the ground level of o-NH_3 – a kinetic temperature of 50 K.[8] The behaviour of the excitation temperature is similar to that of p-NH_3 inversion lines; at low density, it is close to the background temperature, while it is thermalized at densities greater than 10^6 cm^{-3}. We predict, in agreement with Walmsley & Ungerechts (1983), a population inversion for densities ranging between $\sim 4 \times 10^3$ and $\sim 6 \times 10^5$ cm^{-3} (note that the range in which the inversion occurs is slightly different for the two collisional rate sets). This population inversion was first predicted by Walmsley & Ungerechts (1983), and has been studied in detail by Flower, Offer & Schilke (1990). The corresponding maser transition has been since observed in several star-forming regions, e.g. NGC 6334I (Beuther et al. 2007). As explained by

[8] The computations with the rates from the present work do not include the levels above $J = 3$. To make sure that these levels can be neglected at a kinetic temperature of 50 K, we have computed the excitation temperature for the transitions shown in Fig. 7 using Dandy's rates, but without considering the levels above $J = 3$. These were found to be quasi-identical to those computed when the levels above $J = 3$ are considered.

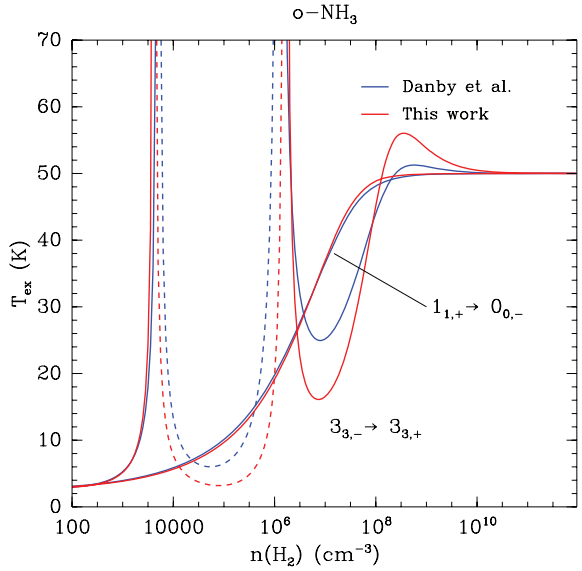

Figure 7. Same as in Fig. 6 for the o-NH_3 $3_{3,-} - 3_{3,+}$ inversion line and for a kinetic temperature of 50 K. The dashed lines indicate negative excitation temperatures.

Walmsley & Ungerechts (1983), the lower level of the transition ($3_{3,+}$) is de-populated by collisions to excited levels in the $K = 0$ ladder, while it is populated by radiative transitions from the $3_{3,-}$ level. For densities greater than $\sim 4 \times 10^3$ cm^{-3}, the collisional de-population rate is greater than the radiative population rate of the lower level, and the inversion occurs. For densities greater than $\sim 6 \times 10^5$ cm^{-3}, excited levels in the $K = 0$ ladder start to become populated and populate the $3_{3,+}$ level collisionally. This limits the maser gain to moderate values; for a density of 1×10^5 cm^{-3}, we predict a negative opacity of only $\tau \sim -2$.

Fig. 7 also shows the excitation temperature of the $1_{1,+} \rightarrow 0_{0,+}$ rotation–inversion transition of o-NH_3. This line, at a frequency of ∼572.5 GHz, was first detected towards OMC-1 with the *Kuiper Airborne Observatory* (Keene, Blake & Phillips 1983). It was also detected towards ρ-Oph A with *Odin* space telescope (Liseau et al. 2003), and will soon be observable with the *Heterodyne Instrument for the Far Infrared* (*HIFI*) on board the *Herschel Space Observatory*. This line is found to thermalize at densities of $\sim 10^9$ cm^{-3}. Once again, little differences between the excitation temperatures computed using the rates of Danby et al. and those from this work are seen. No significant difference was found between the excitation temperatures of the other rotation–inversion transitions that will be observable with *HIFI* either.

4 CONCLUSIONS

We have presented new collisional excitation rates of p- and o-NH_3 with p-H_2($J = 0$). With respect to older computations from Danby et al. (1988), the present rates were found to agree within a factor of 2. In order to investigate the effect of the new rates on the excitation of o-NH_3 and p-NH_3, we have computed the excitation of these species under physical conditions that are typical of dense molecular clouds, pre-stellar cores, as well as the outer envelopes of embedded protostars, using an LVG code. We found that the excitation temperature between the 1_1 and 2_2 levels computed using the new rates is almost identical to that computed using older rates at the low temperatures considered here (≤50 K). Thus, the calibration of the ammonia thermometer appears robust. The effect

of the new rates on the inversion transitions (at cm wavelength) or the rotation–inversion transitions that will be observable with *Herschel–HIFI* is also found to be small.

Future works include extension of the present calculations to p-H_2($J = 0$, 2) and o-H_2($J = 1$) as well as to higher ammonia levels and kinetic temperatures. Comparisons with double resonance (Daly & Oka 1970), crossed beam (Schleipen et al. 1993) and pressure broadening (Willey et al. 2002) experiments will also be investigated, with the objective to establish the predictive ability of the present PES and to distinguish between the predictions of the available PES.

ACKNOWLEDGMENTS

The authors wish to acknowledge their friend and colleague Pierre Valiron who initiated the work that led to this paper. Pierre passed away on 2008 August 31, and he is deeply missed. We also thank Evelyne Roueff for her critical reading of this manuscript. This research was supported by the CNRS national programme 'Physique et Chimie du Milieu Interstellaire' and by the FP6 Research Training Network 'Molecular Universe' (contract no. MRTN-CT-2004-512302).

REFERENCES

Barrett A. H., Ho P. T. P., Myers P. C., 1977, ApJ, 211, L39
Beuther H., Walsh A. J., Thorwirth S., Zhang Q., Hunter T. R., Megeath S. T., Menten K. M., 2007, A&A, 466, 989
Cheung A. C., Rank D. M., Townes C. H., Welch W. J., 1969, Nat, 221, 917
Daly P. W., Oka T., 1970, J. Chem. Phys., 53, 3272
Danby G., Flower D. R., Kochanski E., Kurdi L., Valiron P., 1986, J. Phys. B: At Mol. Phys., 19, 2891
Danby G., Flower D. R., Valiron P., Schilke P., Walmsley C. M., 1988, MNRAS, 235, 229
Daniel F., Cernicharo J., Dubernet M.-L., 2006, ApJ, 648, 461
Davis S. L., Boggs J. E., 1978, J. Chem. Phys., 69, 2355
Davis S. L., Boggs J. E., 1981, J. Chem. Phys., 75, 3937
Faure A., Valiron P., Wernli M., Wiesenfeld L., Rist C., Noga J., Tennyson J., 2005, J. Chem. Phys., 122, 1102
Flower D. R., Offer A., Schilke P., 1990, MNRAS, 244, 4P
Green S., 1976, J. Chem. Phys., 64, 3463
Green S., 1980, J. Chem. Phys., 73, 2740
Ho P. T. P., Townes C. H., 1983, ARA&A, 21, 239
Ho P. T. P., Barrett A. H., Myers P. C., Matsakis D. N., Chui M. F., Townes C. H., Cheung A. C., Yngvesson K. S., 1979, ApJ, 234, 912
Hodges M. P., Wheatley R. J., 2001, J. Chem. Phys., 114, 8836
Hotzel S., Harju J., Juvela M., 2002, A&A, 395, L5
Jankowski P., Szalewicz K., 2005, J. Chem. Phys., 123, 4301
Keene J., Blake G. A., Phillips T. G., 1983, ApJ, 271, L27
Liseau R. et al., 2003, A&A, 402, L73
Machin L., Roueff E., 2005, J. Phys. B: At. Mol. Phys., 38, 1519
Manolopoulos D. E., 1986, J. Chem. Phys., 85, 6425
Mladenović M., Lewerenz M., Cilpa G., Rosmus P., Chambaud G., 2008, Chem. Phys., 346, 237
Morris M., Zuckerman B., Palmer P., Turner B. E., 1973, ApJ, 186, 501
Noga J., Kutzelnigg W., 1994, J. Chem. Phys., 101, 7738
Offer A., Flower D. R., 1990, J. Chem. Soc. Faraday Trans., 86, 1659
Phillips T. R., Maluendes S., McLean A. D., Green S., 1994, J. Chem. Phys., 101, 5824
Pickett H. M., Poynter R. L., Cohen E. A., Delitsky M. L., Pearson J. C., Müller H. S. P., 1998, J. Quant. Spectrosc. Radiat. Transfer, 60, 830
Rajamäki T., Kállay M., Noga J., Valiron P., Halonen L., 2004, Mol. Phys., 102, 2297
Rist C., Alexander M. H., Valiron P., 1993, J. Chem. Phys., 98, 4662
Schleipen J., ter Meulen J. J., Offer A. R., 1993, Chem. Phys., 171, 347
Schöier F. L., van der Tak F. F. S., van Dishoeck E. F., Black J. H., 2005, A&A, 432, 369
Scifoni E., Valiron P., Faure A., Rist C., 2007, in Lemaire J. L., Combes F., eds, Molecules in Space and Laboratory. S. Diana, p. 127
Troscompt N., Faure A., Wiesenfeld L., Ceccarelli C., Valiron P., 2009, A&A, 493, 687
Valiron P., Wernli M., Faure A., Wiesenfeld L., Rist C., Kedžuch S., Noga J., 2008, J. Chem. Phys., 129, 134306
van der Sanden G. C. M., Wormer P. E. S., van der Avoird A., Schleipen J., Ter Meulen J. J., 1992, J. Chem. Phys., 97, 6460
van der Tak F. F. S., Black J. H., Schöier F. L., Jansen D. J., van Dishoeck E. F., 2007, A&A, 468, 627
Walmsley C. M., Ungerechts H., 1983, A&A, 122, 164
Willey D. R., Timlin R. E. Jr., Merlin J. M., Sowa M. M., Wesolek D. M., 2002, ApJS, 139, 191

This paper has been typeset from a TEX/LATEX file prepared by the author.